

A COMPARISON OF WINDS MEASURED BY
A 915 MHZ WIND PROFILING RADAR AND A DOPPLER LIDAR

William J. Shaw*
Pacific Northwest National Laboratory
Richland, Washington

Lisa S. Darby and Robert M. Banta
NOAA Environmental Technology Laboratory
Boulder, Colorado

1. INTRODUCTION

Recent work has suggested that it may be possible to extract much higher quality wind information from wind profiling radars than we have traditionally expected. In particular, Gossard et al. (1998) suggested that selection of Doppler spectral peaks by a “human expert” combined with suitable data processing could yield accurate estimates of wind profiles over periods as short as a few minutes. This is in marked contrast to the traditional consensus averaging approach to wind profiler data that yields wind profiles for periods usually no shorter than 30 min. Nearly coincident with that work, the National Center for Atmospheric Research (NCAR) has developed the NCAR Improved Moment Algorithm (NIMA: Cornman et al. 1998; Cohn et al. 2001; Morse et al. 2002; Goodrich et al. 2002), which uses a combination of fuzzy logic and pattern recognition algorithms to emulate peak selection by a human expert. In this paper, we compare profiler winds derived from NIMA processing with those from a Doppler lidar system operated by the National Oceanic and Atmospheric Administration (NOAA).

An opportunity for comparison of these systems occurred in October 2000, when the U.S. Department of Energy supported a month-long field study in the Salt Lake Valley. The purpose of the campaign was to investigate the physical processes associated with the dispersion of pollutants in stably stratified urban basins. The Vertical Transport and Mixing (VTMX) field work is described in Doran et al. (2002). As part of this study Pacific Northwest National Laboratory (PNNL) operated a 915 MHz wind profiling radar in the central Salt Lake Valley. During the same period NOAA’s Environmental Technology Laboratory (ETL) operated a Doppler lidar system in a variety of scanning modes. One of these modes was intended to provide a direct comparison with short-term winds from the profiler.

2. INSTRUMENTATION

Figure 1 shows the relative locations of PNNL’s wind profiler and NOAA/ETL’s lidar system in the Salt Lake Valley. This valley has relatively gentle slopes for a radius of roughly 10 km from its center. It opens in the north-northwest to the Great Salt Lake. The Wasatch

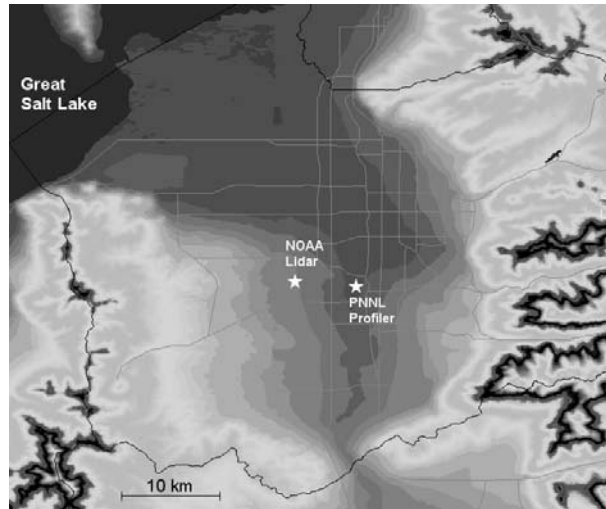


Figure 1. Salt Lake Valley, Utah, showing the relative locations of the Doppler lidar and wind profiling radar.

Range rises sharply on the east side of the valley, and the Oquirrh Mountains form a prominent barrier to the west. In the south, the Traverse Mountains form a southern boundary between the Salt Lake Valley and Utah Valley. The profiler was located very near the center of the Salt Lake Valley at an elevation of 1310 m MSL. The lidar was sited 7.25 km from the profiler at Municipal Airport No. 2 at an elevation of 1410 m MSL. The bearing from the lidar to the profiler was 96.6°.

2.1 PNNL Wind Profiler

The wind profiling radar is a 915 MHz phased array system manufactured by Radian Corp. (now Vaisala). During the campaign, it was set to alternate between a five-beam low-mode, with 60 m range-gate resolution, and a five-beam high mode, with 200 m range gates. For 5 min each half-hour, the system measured temperature using its Radio Acoustic Sounding System (RASS) mode. The beams consist of one vertical and two orthogonal pairs of opposing off-zenith beams at a zenith angle of 23.6°. We found that, despite the additional power of the high mode, the low mode performed as well within the boundary layer, and both modes provided little information above it. Because of the higher vertical resolution of the low mode, we’ve confined our attention to it. The velocity precision of this

*Corresponding author address: William J. Shaw, Pacific Northwest National Laboratory, PO Box 999, MS K9-30, Richland, WA 99352. e-mail: will.shaw@pnl.gov.

instrument using normal consensus processing has been determined to be 1 m s^{-1} (Martner et al. 1993).

The profiler completed one cycle through the beams of each mode roughly every 3.5 min. Thus, NIMA is able to construct a low-mode profile of the horizontal wind vector once every 7 min. In addition to the winds, NIMA also provides a confidence estimate [0...1] for each component, where 0 represents no confidence and 1 is perfect confidence. We have used these estimates as described below to filter *a priori* the profiler winds included in the comparison.

NIMA also produces consensus winds in which moments that are not judged to be outliers are averaged over a specified interval. The vector winds at each range gate are then calculated from the averaged moments. For comparison with the velocity-azimuth display (VAD) vector wind profiles derived from the lidar, we have used 30-min consensus winds from the profiler.

2.2 NOAA Doppler Lidar

The NOAA/ETL lidar deployed at VTMX, TEACO₂, is a pulsed Doppler system that emits a narrow beam of eye-safe light, $\sim 1 \text{ m}$ across at 11 km range, at a wavelength of $10.59 \mu\text{m}$. From the lidar's location at the Salt Lake City Municipal Airport #2, measurements of radial velocity and backscattered signal intensity spanning the basin were acquired during nine intensive operating periods (IOPs) of the VTMX field campaign. A Doppler lidar is a clear-air remote sensor. With a normal distribution of atmospheric aerosols, most of the backscattering occurs by particles $1\text{--}3 \mu\text{m}$ in diameter. The clear air returns, combined with the fact that there is no ground-clutter, make Doppler lidar an excellent instrument for measuring winds in complex terrain (for example, see Banta et al. 1995, Darby et al. 1999, and Flamant et al. 2002). In order to minimize blockage of the lidar beam by terrain, it was necessary to site the lidar at an elevation higher than that of the profiler, hence the elevation difference between the PNNL profiler and the Doppler lidar.

During VTMX, the NOAA/ETL lidar operated with a pulse repetition frequency of 10 Hz , and every 3 pulses, or beams, were averaged together. The technical aspects of TEACO₂ were described by Post and Cupp (1990), including an estimate of the velocity precision, which was 60 cm s^{-1} . The along-beam data were binned into 300 m range gates. The minimum range is 1.2 km , and during VTMX the maximum range varied between 10 and 20 km depending on how much aerosol was in the basin. The maximum range was often several kilometers greater in the lowest 500 to 1000 m of the scan volume. The scanning rate varied between 1° and 3° s^{-1} , depending on the spatial resolution desired for a given scan.

The data acquisition routine included a sequence of scans that alternated between constant-elevation angle scans, called Plan-Position Indicator (PPI) scans, and constant-azimuth angle scans, called Range-Height Indicator (RHI) scans. Sets of these scans lasted just under an hour. Scans could be added in real time to document wind features of interest as they occurred.

Minimum Beam Elevation	Maximum Beam Elevation	Elevation Change between Sweeps
-0.5	3.0	0.5
5	15	5
30	45	15

Table 1. PPI scan volumes for NOAA Doppler lidar.

The RHI scans used for the lidar-profiler comparisons were taken along the the 96° radial (relative to the lidar) from -1° to 30° in elevation, at a scanning rate of 1° s^{-1} , thus taking 31 s to complete. RHI scans were used to detect layers of wind shear, both directional and speed.

The radial velocity data from the 96° RHI scans used for the lidar-profiler comparisons were transformed from polar to Cartesian coordinates. The grid spacing of the Cartesian grid was 0.15 km along X and 0.015 km along Z, with X defined as the horizontal distance from the lidar, and Z defined as the distance above the lidar. A radius of influence of 0.5° in elevation and 0.45 km along the beam was used; thus, some smoothing was included in the gridding process. After gridding, the horizontal component of the wind parallel to the plane of the RHI was computed by dividing radial velocities by the cosine of the elevation angle of the lidar beam. The lowest 5 rows (0.075 km) of the grid were flagged as bad due to hard-target contamination. The horizontal component of the wind was then filtered using a uniform filter, in which all data are weighted equally, and the filter is performed over regions that are 3×3 grid points in size.

The PPI scan volumes for VTMX are shown in Table 1. The PPI scans below 3° elevation did not have full 360° azimuthal coverage due to blockage of the beam by terrain, buildings, etc. PPI scans were used to measure the across-basin variability in the winds, including the horizontal structure of the canyon outflows and the along-basin jet.

For PPI scans with an elevation angle $\geq 2.5^\circ$ and $\leq 30^\circ$, the Velocity-Azimuth Display (VAD) method (Browning and Wexler, 1968) was used to produce vertical profiles of the horizontal wind. For a full 360° scan, each range gate (300 m in length) produces a ring of data. Calculations were performed for each ring, or the n^{th} range gate of each beam. In this case, we used $n = 4$ to 83 (or 1.2 km to 25 km range along the beam). The velocity data for each ring are fit to a sine curve, with outliers eliminated, and a wind speed and direction are calculated by the amplitude and phase, respectively, of the sine curve. The elevation angle is used to calculate the height above the lidar of the wind speed and direction, as well as the horizontal component of the wind. The combination of the narrow lidar beam, the three-beam averaging, and the scanning rate make it very unlikely that the motion of birds or insects in flight would contaminate the Doppler lidar measurements.

3. APPROACH FOR COMPARISON

The lidar can measure only radial velocity in an RHI scan. Therefore, to achieve a comparison, we projected

the horizontal wind vectors from the profiler onto the 96° bearing of the lidar beam:

$$v_r = u \sin \beta + v \cos \beta \quad (1)$$

where β is the bearing angle of the lidar beam and u and v are east and north components of the profiler winds respectively. We used a weighted geometric average of the NIMA wind component confidence estimates to eliminate profiler winds from the comparison. The weighting was determined by the magnitude of the projection of each component onto the lidar radial direction:

$$C = \exp\left(\frac{|\sin \beta| \ln C_u + |\cos \beta| \ln C_v}{|\sin \beta| + |\cos \beta|}\right) \quad (2)$$

where C is the weighted confidence, and C_u and C_v are the confidence estimates for each component. We did not include winds for values of $C < 0.4$.

Because the lidar and radar sampling was performed over different space and time intervals, it was necessary to average data to provide comparison points. The lidar completed an RHI scan from which its radial velocities were derived in about 30 s. Occasionally two of these scans would be done in an interval of a few minutes, but in general these were single scans separated by many minutes or hours. If two scans occurred in rapid succession, we averaged them for comparison with the temporally nearest 3.5-min radar profile. The vertical resolution of the gridded lidar data was 15 m while the vertical resolution for the profiler winds was 55 m. (This is slightly less than the range-gate spacing because of the projection of the off-zenith beams onto the vertical.). Therefore we also averaged the lidar data in the vertical to obtain values corresponding to each profiler range gate. We subtracted 110 m from the profiler range gate values to account for the elevation difference between the two sensors.

For comparisons of VAD wind vector profiles derived from the lidar's PPI scans, we employed a similar procedure. In this case, it was common for the lidar to execute several scans at different elevation angles separated by only a few minutes. These clusters of scans were then separated from other clusters by the order of an hour during the IOPs. Unlike the gridded radial velocity data, which were essentially profiles at a point, the VAD winds represented averages over a considerable area. As a result, it seemed more appropriated to compare VAD scans to profiler wind from the NIMA consensus algorithm for periods of 30 min rather than 3.5 min. To obtain data for comparison, we vertically averaged all VAD profiles that fell within a profiler consensus interval so that VAD winds matched the profiler range gates. The separate VAD profiles were then averaged to create a single profile corresponding to the radar's data. Data from the profiler were included in this case only if the NIMA

confidence estimates for both components exceeded 0.4.

4. RESULTS

4.1 Short-term Radial Velocities

The RHI lidar scans in the direction of the PNNL profiler yielded 30 profiles for comparison during VTMX. The comparisons ranged from remarkably good to very different. Figure 2a shows one of the excellent comparisons of radial velocity. The profiles from the two instruments in this case are nearly indistinguishable. Figure 2b, on the other hand, shows pronounced disagreement between the two systems, especially in the upper part of the profile.

It is somewhat perplexing that the two systems could show such excellent agreement in some cases and such poor agreement in others. We are currently pursuing the causes of this behavior. One obvious possibility is that NIMA is successful in recognizing the pattern of spectral moments in some cases but settles on the wrong pattern in others. This possibility ought to be minimized by our use of the confidence criterion, but we will need to examine a number of individual spectra

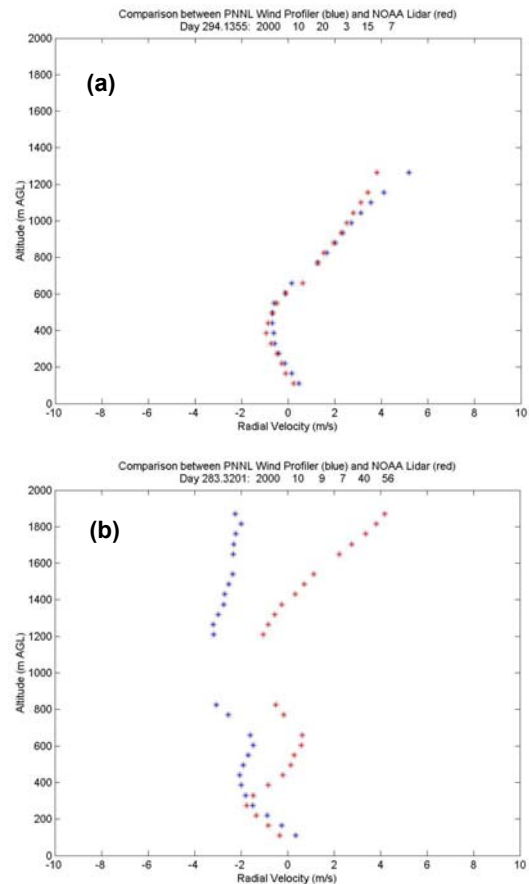


Figure 2. (a) Example of an excellent radial velocity comparison between the lidar and the profiler. (b) Example of a poorer comparison.

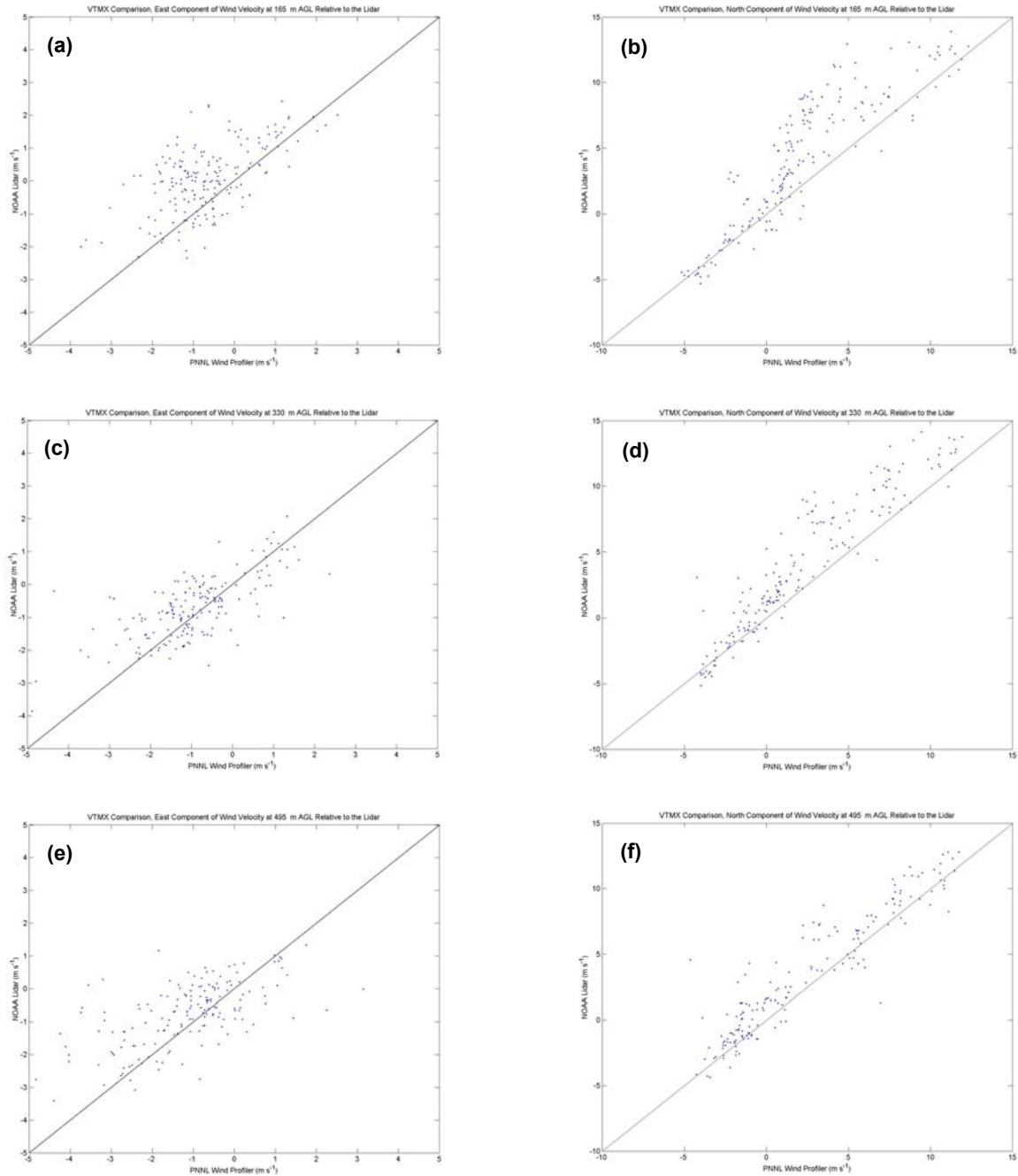


Figure 3. Comparison between u - and v -components from 30-minute profiler consensus values and corresponding VAD winds from the Doppler lidar. (a) and (b) are from 165 m above the lidar, (c) and (d) are from 330 m, and (e) and (f) are from 495 m.

to be sure. It is also possible that differences arose because of factors other than faulty instrument performance. One candidate culprit is birds. All of the profilers in VTMX exhibited spurious north winds and anomalously high signal-to-noise ratios at night, especially above 1000 m. That we were measuring in October suggests that the fall migration may be responsible. The lidar is not affected by migrating birds.

At times the disagreement is due to strong, small-scale horizontal variations in the wind field. PPI scans from the lidar (not shown) indicate that thin flow layers were often present, and slope and canyon outflow from the Wasatch Range to the east, which were sampled differently by each instrument, can cause differences in the wind profiles. The 0.6° difference between the lidar beam direction and the actual direction from the lidar to

the profiler yields a spatial separation of 75 m between the profile locations at 7.25 km. With sharply varying wind fields, this was often significant. Spatial and temporal variations in the wind field in complex terrain as a source for discrepancies between two measurement systems (Doppler lidar and airborne measurements) were discussed by Durran et al. (2003).

4.2 VAD-Consensus Comparison

There were many more VAD scans during VTMX than RHI scans directed toward the PNNL profiler. We have therefore used scatterplots rather than individual profiles to compare these data. Figure 3 compares wind components from the profiler and the lidar at three separate altitudes below 1 km. Data are included from all times during VTMX. Because of the pronounced diurnal cycle of up- and down-valley flow, the v-component is frequently of much larger magnitude than the u-component.

Figure 3a shows the u-component at a height of 165 m AGL relative to the lidar. The profiler tends to have a negative bias of about 1 m s^{-1} . The v-component, on the other hand shows excellent agreement for negative values (up-valley flow) but a distinct negative bias in the radar for positive values (Fig. 3b). At 330 m, the behavior of both components is similar to the lower altitude (Figs. 3c and 3d). However, the correlation between the u-component estimates is a little better and the negative bias in the radar for positive v-components is not quite so pronounced. At 495 m (Figs. 3e and 3f) the comparison for u continues to show scatter, but the negative bias in the radar is much less.

The above behavior is intriguing and may reveal more about the local meteorology than instrument behavior. Because the sampling volume for the two systems was very different in this case, we were not surprised that there was some scatter in the comparison. The negative bias in the positive v-component from the radar may be indicative of a characteristic nocturnal flow in the Salt Lake Valley. The Traverse Mountains in the south end of the valley have a gap, known as the Jordan Narrows, through which the Jordan River flows. It is common for strong south winds to develop in this gap at night, and these winds flow into the Salt Lake Valley as a jet several hundred meters deep. Given the 7.25 km separation between the profiler and the lidar, it is quite possible that the jet exerts more influence at the lidar site. The existence of a near-surface jet is also consistent with the fact that the radar negative bias diminishes with height.

5. SUMMARY

We have compared short-term radial velocities from a Doppler lidar and a 915 MHz wind profiling radar in the Salt Lake Valley, Utah. Short-term (3.5-min) velocity profiles from the radar were computed using the NCAR Improved Moment Algorithm. While comparisons showed substantial disagreement in cases that we continue to explore, some of the profiles agreed spectacularly well, suggesting that with careful

processing wind accuracies on the order of a few 10 's of cm s^{-1} are possible over very short periods from these systems.

We have also compared half-hour consensus values with VAD winds from the lidar. There was broad agreement between the two systems, but within considerable scatter. This scatter is not too surprising, given the terrain-induced spatial variability of the wind field in the Salt Lake Valley. An interesting result is that the data suggest that the lidar was more directly affected by a southerly jet that frequently developed through the Jordan Narrows at night.

6. CONCLUSIONS

For periods of time the wind component profiles derived from lidar vertical-slice scans and the profiler seemed to agree to better than the published accuracy of either instrument. Such agreement is the more remarkable, because the scattering targets in each case are different—aerosol for the lidar and temperature and humidity fluctuations for the profiler. These periods occurred when each instrument was sampling at high SNR and when the wind field in the vicinity of the profiler was relatively uniform.

Periods when the agreement was not so good occurred when the wind field was spatially variable near the profile or when various instrumental problems occurred. In several instances azimuth scans from the Doppler lidar documented slope flows or even stronger canyon outflows from the east penetrating to the location of the profiler, resulting in strong horizontal variability and vertical layering of the flow. The horizontal variability was sampled differently by the two instruments, producing discrepancies in the measured profiles. Vertical layers of easterly canyon outflow of less than 300-m depth were sampled by lidar RHI scans but not by the profiler, also causing disagreement. This clear documentation of spatial heterogeneity as a cause of discrepancy between the two instruments is a significant result of this study. Although it is often asserted that spatial variability is a cause of measurement uncertainty, measurements showing this effect unequivocally are rare.

Instrumental issues producing uncertainty include low SNR for either instrument, migrating birds for the profiler, and the velocity estimation algorithm choosing the wrong peak in the Doppler spectrum during processing.

7. ACKNOWLEDGEMENTS

This work was supported by the U.S. Department of Energy (DOE), under the auspices of the Atmospheric Sciences Program of the Office of Biological and Environmental Research. We are grateful to NCAR for providing NIMA to PNNL through a research license and for helpful discussions with Cory Morse of NCAR and Chris Doran of PNNL. We are also indebted to Cui-Juan Zhu of NOAA/ETL for processing the gridded lidar data. This work was performed at Pacific Northwest National Laboratory, which is operated for DOE by the Battelle

Memorial Institute under contract DE-AC0676RLO 1830, and at NOAA/ETL.

8. REFERENCES

- Banta, R. M., L. D. Olivier, W. D. Neff, D. H. Levinson, and D. Ruffieux, 1995: Influence of canyon-induced flows on flow and dispersion over adjacent plains. *Theor. Appl. Climatol.*, **52**, 27-42.
- Browning, K.A., and Wexler, R., 1968: The determination of kinematic properties of a wind field using Doppler radar. *J. Appl. Meteor.*, **7**, 105-113.
- Cohn, S. A., R. K. Goodrich, C. S. Morse, E. Karplus, S. W. Mueller, L. B. Cornman, and R. A. Weekley 2001: Radial velocity and wind measurement with NIMA–NWCA: Comparisons with human estimation and aircraft measurements. *J. Appl. Meteor.*, **40**, 704–719.
- Cornman, L. B., R. K. Goodrich, C. S. Morse, and W. L. Ecklund 1998: A fuzzy logic method for improved moment estimation from Doppler spectra. *J. Atmos. Oceanic Technol.*, **15**, 1287–1305.
- Darby, L. S., W. D. Neff, and R. M. Banta, 1999: Multiscale analysis of a Meso- \exists frontal passage in the complex terrain of the Colorado Front Range. *Mon. Wea. Rev.*, **127**, 2062-2081.
- Doran, J. C., J. D. Fast, and J. Horel 2002: The VTMX 2000 campaign. *Bull. Am. Meteorol. Soc.*, **83**, 537-551.
- Durrán, D. R., T. Maric, R. M. Banta, L. S. Darby, and R. M. Hardesty 2003: A comparison of ground-based Doppler lidar and airborne in situ observations above complex terrain. *Quart. J. Roy. Meteor. Soc.*, in press.
- Flamant, C., P. Drobinski, L. Nance, R. Banta, L. Darby, J. Dusek, M. Hardesty, J. Pelon, and E. Richard, 2002: Gap flow in an Alpine Valley during a shallow south foehn event: Observations, numerical simulations, and hydraulic analog. *Q. J. R. Meteorol. Soc.*, **128**, 1171-1210.
- Goodrich, R. K., C. S. Morse, L. B. Cornman, and S. A. Cohn 2002: Horizontal wind and wind confidence algorithm for Doppler wind profilers. *J. Atmos. Oceanic Technol.*, **19**, 257–273.
- Gossard, E. E., D. E. Wolfe, K. P. Moran, R. A. Paulus, K. D. Anderson, and L. T. Rogers 1998: Measurement of clear-air gradients and turbulence properties with radar wind profilers. *J. Atmos. Oceanic Technol.*, **15**, 321–342.
- Martner, B. E., D. B. Wuertz, B. B. Stankov, R. G. Strauch, E. R. Westwater, K. S. Gage, W. L. Ecklund, C. L. Martin, and W. F. Dabberdt 1993: An evaluation of wind profiler, RASS, and microwave radiometer performance. *Bull. Am. Meteor. Soc.*, **74**, 599–613.
- Morse, C. S., R. K. Goodrich, and L. B. Cornman 2002: The NIMA method for improved moment estimation from Doppler spectra. *J. Atmos. Oceanic Technol.*, **19**, 274–295.
- Post, M.J., and R.E. Cupp, 1990: Optimizing a pulsed Doppler lidar. *Appl. Opt.*, **29**, 4145-4158.